THE OPTICAL SYSTEMS OF LHCb RICHes: A STUDY ON THE MIRROR WALLS AND MIRROR SPECIFICATIONS

C. D'Ambrosio, L. Fernandez, M. Laub, D. Piedigrossi
CERN, 1211 Geneva, Switzerland

INTRODUCTION

The LHCb detector is developed and constructed for the LHC project at CERN. For its particle identification sub-detectors, it features two Ring Imaging CHerenkov detectors. Major components are their mirrors together with all the required structures to achieve proper alignment and optical resolution. In the following, we describe in short the optical systems of both RICHes and the procedures for their survey and alignment. Then, we discuss what are the major considerations for the mirror choice. Their specifications are given together with the results achieved on several prototypes through a collaboration program with industry. Finally, the experimental set-ups developed and realized to precisely characterize mirrors optical properties are described in detail and they will serve for the final mirror qualification.

I THE OPTICAL SYSTEM OF LHCb RICHes

The radiator of RICH-2 will consist of 1.7 m on average of CF_4 gas. Its optical system is composed of two spherical mirror walls, with 8 m radius of curvature and both tilted of 450 mrad, to bring the image out of the spectrometre acceptance. In order to stay into a total thickness for RICH-2 of 2.1 m, two flat mirror walls are needed, each tilted of 140 mrad with respect to the beam axis (Fig. 1). The photodetector entrance plane is placed at 4 m from the spherical mirror walls. The overall precision per detected photon is expected to be 0.35 mrad [1]. For RICH-1, the gas radiator length is 0.85 m and the mirror radius of curvature is 1.7 m. The spherical mirror walls are tilted of 250 mrad with respect of the beam axis and face directly the photodetector planes. The expected precision per detected photon is 1.1 mrad [1].

II PROCEDURE FOR WALL SURVEY AND ALIGNMENT

The spherical and plane mirror walls of RICH-2 will have to be precisely aligned in order to obtain the required resolution on the Cherenkov rings and to fully exploit the photodetector capabilities. Each spherical and flat mirror has to be aligned with respect to the other mirrors to form spherical and plane walls (Fig. 1). They must have their centers of curvature[1] pointing to the center of the photodetector. The spherical and flat walls have therefore to be aligned one with respect to the other and both with respect to the particle beam axis. The optical alignment will be first carried out in a suitable laboratory and will be checked once, when the RICH-2 is lowered and placed in the experimental area. Reasons, which make unreasonable a complete survey and alignment in the pit, are given by lack of space and by dust in the pit, by the large radius of curvature of the mirrors, by the flat-spherical walls and by the wafer-thin geometrical shape of RICH-2.

The optical alignment procedure can be summarized as following: first, the superstructure is surveyed and reference axes and focal points are defined, as well as the position of the mirror support walls. Then the spherical walls are aligned with respect to the focal points, without the flat walls and by means of a laser point source (Fig. 2). At this point, the flat walls are mounted and the point source is moved into a point situated roughly on the particle beam axis. The flat and spherical walls are then aligned to generate a single image point on the axis normal to the photodetectors plane (Fig. 2). This will allow also a measure of the total astigmatism of the system. When the RICH-2 detector is lowered in the pit and placed on the beam axis, this last step will be repeated, to check and correct eventual misalignments. The overall alignment error[2] foreseen is set solely by the survey (± 1 mm shift on the photodetector plane) and by the precision of the optical mounts. The spherical- and flat- mirror resolution and the mount precision will set the overall resolution of the optical system:

[1] For the flat walls this is the axis normal to the plane.
[2] It is worth noting the difference between alignment error and optical resolution of the system.

$\approx 2.36\sqrt{2 \cdot 0.24^2 + 2 \cdot 0.12^2} = 2.36 \cdot 0.38\, mm$ at FWHM, where we have considered a s = 0.03 mrad precision for each optical component[3].

III CONSIDERATIONS ON MIRROR CHOICE

To efficiently cover a certain surface with an array of mirrors, we need to establish a relation between their physical qualities (material, shape, size, thickness and weight), their optical qualities (geometrical precision and reflectivity) and the characteristics of the formed array (number of mirrors, complexity, overall weight and fraction of radiation lenght) and cost.

Mirrors in RICH detectors must represent a small fraction of the whole material budget. In RICH-2, for example, the upper limit is established around 5÷6 % of their radiation length X_0. In the past, mirrors have been produced out of glass, glass and glass-foam, glass and composites, plastic and composites and, for RICH-1, we are also considering a recently established glass and beryllium technique [2]. Present and future RICH mirrors are somewhat defined by the photodetector choice, in the sense that their reflective layer will have to cover a more or less wide region in the ultraviolet spectrum, according to a choice of a gas-based or a solid-state vacuum photodetector. For the LHCb RICHes, the choice is for vacuum phototubes, which allows the use of relatively standard reflective coatings. Fluctuation in the value of the radius of curvature will play a lesser role than its average angular fluctuation.

All the following discussion is focussed mainly on the spherical mirror walls. However, most of the considerations are valid also for the flat mirrors. They will be most probably of rectangular shape and of the same thickness as the hexagonal mirrors. With flat mirrors a complication arises from the fact that they do not have a finite focal plane and therefore both the definition and the measurement of the average angular precision have to be redefined to some extent. This point will be addressed in the experimental set-ups section.

[3] As we shall see in the next section, the physical quantity is $D_0 = 4s$; nevertheless we shall continue to

The number of mirrors (N_m) covering the surface has to be kept as small as possible to reduce complexity, optical tests and costs. The lower limit for N_m will be set by:

- Their maximum acceptable thickness X_m (in unit of X_o), which has to increase with their radius r_m in order to retain their optical properties. These are essentially given by the radius of curvature R = 8 m and the average angular precision, set to $s_J \approx 0.03$ mrad, to not affect the overall detector resolution of ~2.5 mm (see Sect. II).

- The mirror weight, which has to be acceptable for the mount. This is made of Polycarbonate to keep X_{mount} low (~5% X_o) and similar to the support wall (4 % X_o) in which it is inserted [3]. Long term stability [4] and mount alignment precision [5] were demonstrated for a weight of ~2 kg, which sets the maximum acceptable mirror radius to 230 mm for a thickness of 6 mm. Future measurements should demonstrate same behaviour for ~3 kg weight mirror, that is a mirror inscribed in a circle of ~250 mm radius and with a 7 mm thickness.

Another important parameter to take in account is given by the ratio between the maximum base radius (r_c) of the Cherenkov cones on the mirrors and the mirror radius r_m. As the gas thickness is relatively short (~1.7 m) and $q_{max} \cong 32$ mrad, then $r_c = 1.7 q_{max} \cong 55$ mm and $p_c = (r_c / r_m) = 22$ %, where p_c gives the probability of having a ring imaged by more than one mirror and $r_m \cong 250$ mm. To have most of the rings imaged each by one mirror, provides us with an easier pattern recognition and correction in case of mirror misalignments.

In view of these basic elements, we aim for RICH-2 at hexagonal glass mirrors inscribed in a radius of 251 mm [3] and thickness between 6 and 7 mm. As we will show later, this thickness is sufficient to ensure the average angular precision of s_J = 0.03 mrad, whilst the long term stability of s_J has yet to be demonstrated. For RICH-1, rectangular mirrors with roughly the same size but thinner (~5 mm) seem to be feasible, as their radius of curvature is only 1.7 m, therefore making them intrinsically more stable. For RICH-1 mirrors made of a Beryllium- or a composite-

---

use s, in order to have an estimation for the calculation of precision.

substrate and a thin glass layer worked to the required precision are also being investigated. Their evident advantage is the low fraction of X_o (~2% X_o).

IV MIRROR SPECIFICATIONS AND EXPERIMENTAL SET-UPS

Mirror parameters are being partially determined on the basis of measurements on mirror prototypes. Further, to ensure the needed quality, mirror specifications have to be verified by measurements. It is planned to check the most critical specifications on all the mirrors, that is:

- Visual inspection, to assess cracks, bubbles, etc.;
- Dimensions;
- Average value R of radius of curvature;
- Average angular resolution;
- Average reflectivity.

In the EP/TA2 optical laboratory, set-ups are already prepared or under preparation to carry out these checks. In the following, they are described and the first results are discussed.

IV-1 The set-up for spherical mirror radius of curvature and average geometrical quality measurement

Each spherical mirror will be tested on radius of curvature and average geometrical quality[4] before installation inside the RICH vessel. The measurement set-up is fully operational. Because of similar characteristics of LHCb RICH-2 and COMPASS RICH-1 mirrors [6], some results obtained from measurements on the first COMPASS RICH mirrors, published in [7], are also described.

The set up (Fig. 3) measures the rms variation from the ideal mirror spherical surface by imaging a point source via the sample mirror and by analyzing the size and shape

[4] We shall see that the average geometrical quality is evaluated by the average angular precision s_J

of the resulting focal spot. A diode-laser beam at 641 nm (a) is injected into a mono-mode optical fiber (b). Modes are excited in the fiber to obtain a uniform point-like source (c) at its output, less than 10 μm diameter. Inside the numerical aperture of the fibers, the intensity on spherical surfaces pointing to the source is constant and decreases as $1/R^2$, where R is the radius of the sphere. Therefore, this light illuminates uniformly the mirror (d) and is focussed back. A CCD camera (e) is placed in the focal plane to obtain an image of its intensity distribution. The average radius of curvature of the i-th mirror is measured by $2/R_i = 1/d_{1i} + 1/d_{2i}$, where $d_{1,2i}$ is the distance between point-source-mirror and mirror-focal plane respectively. R_i is obtained by finding the focus (that is the smallest possible spot) on the CCD camera by varying d_{2i}. Point source and CCD camera move together, therefore d_{1i} equals d_{2i} when we are in the focal plane. Focal plane and radius of curvature R plane coinciding, the measurement is spherical aberration-free.

From measuring N mirrors, we will obtain a distribution in R. For RICH-2, its standard deviation should not exceed

$$\sigma_R = \frac{\sigma_d}{r_c - \sigma_d} R \sim 1.0\% R$$

where s_d is the photodetector precision and r_c the Cherenkov cone base radius.

If the mirror had a perfect spherical surface, the spot on the focal plane should have had same dimensions at the point source. However, geometrical distortions[5] can be present for mirrors with large surfaces (≥ 0.10 m^2) and thin substrates (≤ 7 mm). The net result is an enlargement of the focal spot with the presence of irregularities on the borders (Fig. 4). In term of wave optics, the image of the point source is described by a complicated Fresnel diffraction integral, representing an optical system made of an imperfect lens and an hexagonal pupil, in principle far from a monotonic bidimensional distribution [8,9]. This complication can be easily appreciated by looking at Fig. 4. On these bases, we define D_0 as the diameter of the circle which

[5] To be distinguished from polishing imperfections, which greatly depend on the hardness of the substrate and also generate poor optical quality.

contains 95% of the total intensity of the spot distribution in the *R* plane for a certain mirror and centered at the centre of gravity of the spot. We also define a $\sigma_s = D_0/4$, which would represents the rms value of the distribution, if this were of gaussian shape. It can be demonstrated that

$$\sigma_\vartheta = \frac{\sqrt{\sigma_s^2 - \sigma_p^2}}{2R} \approx \frac{\sigma_s}{2R} = \frac{D_0}{8R} \qquad (1)$$

where the factor 2 in the denominator takes in account a mirror reflection, s_J is the rms value of the radius of curvature values taken over the mirror surface and expressed in radians[6] and $s_{s,p}$, the rms values for the spot size and the source size, respectively. It follows that we can require D_0 and *R* to be integral parts of each mirror specifications and verify by measurements their values.

When we talked of "smallest possible spot", we avoided to define what smallest means. Presently, we do on the basis of the previous definition of s_s, in the sense that it has to be the smallest of a set of $D_0(d) = 4\,s_s(d)$ obtained varying *d*.

To check in a precise and automatic way this specification, we have developed a computer program, which measures the quantity of light inside a circle with diameter *D* with respect to the total light intensity inside the CCD active area. The program first positions camera and point source at a distance *d*, by means of a computer controlled stepping motor (Fig. 3). Then it takes an image (Fig. 4), in which it finds the center of gravity of the spot and then performs the analysis up to a D_{max} equal to the size of the CCD camera. The resulting curve versus diameter provides the data necessary to the determination of $D_0(d)$ and $R(d)$, Fig. 5. At this point, the distance *d* is changed and the process restarts. When the quantity $min(D_0(d))$ is found, the corresponding *R* is defined as the radius of curvature, Fig. 6. For flat mirrors, the set-up needs to be slightly modified, as shown in the insert of Fig. 3.

[6] We stress the fact that s_J here differs by a factor ½from the angular resolution as defined in the LHCb Technical Proposal [1].

It is worth noting that D_0 is independent from the spot shape and distribution. This is not the case for the precision s_J, where we suppose – or impose – a radial symmetry for the spot. This is why s_J cannot be strictly interpreted as a rms value of a distribution and, therefore, the value required to be satisfied on the mirror specifications will be D_0.

IV-1-1 Experimental results

We have tested forty RICH mirror prototypes for both the LHCb and COMPASS RICH detectors. On the basis of the obtained results, we provided feedback to the mirror manufacturers. The first prototypes were mostly not satisfying, but the latest ones are good and they can give us an idea of the achievable parameters.

Results on the average angular precision (average geometrical quality) together with mirror basic parameters are presented in Table 1. Mirrors had circular or hexagonal shape with circumference diameter from 300 to 600 mm and thickness from 6 to 50 mm. They were simple-glass type mirrors made of Pyrex or Simax glass, apart of OMEGA mirrors [10], which consisted in a glass-sandwiched glass-foam with total thickness 50 mm. Radius of curvature varied from 6.6 to 10.0 m. Some of the mirror substrates were not coated. This does not affect the measurement of the geometrical quality of the substrate.

A requirement of s_J = 0.03 mrad on the mirror average geometrical quality would be fulfilled by the COMPASS prototype No. 5. The thickness of this prototype was 7.5 mm. We obtained more significant data from the measurement of the first ten final COMPASS mirrors. Results on measurement of the average geometrical quality are shown in Fig. 7, together with results on the measurement of radius of curvature in Table 2. From these results we can see what dispersion of values for R and for s_J we can expect. Sigma for the fluctuation of the radius of curvature was approximately s_R = 25 mm, four sigmas representing 1.5 % of the average radius of curvature value. The average s_J was 0.045 mrad. The spot images, corresponding to mirror No. 9 and mirror No. 2 are shown in Figs 8a and 8b respectively. The results were slightly

affected by the fact that mirrors were cut twice to smaller diameter. This operation was avoided in case of the COMPASS mirror No. 0 (Fig. 9). It is inside LHCb RICH-2 requirements and has a thickness of only 6 mm. From this mirror we determined the measurement precision for *R* (Fig. 6) and we also checked the possible influence of the mirror mount used in the set-up. Results from repeated measurement (Table 3), each at different position of the mirror on the three-point support, show that the fluctuation of the radius of curvature was 2.1 mm, consistent with the obtained precision s_R and that the fluctuation for s_J in the various positions was 0.003 mrad. A definite assessment of s_J can be only given when this is measured on the final mount.

We measured also prototypes of LHCb RICH-2 mirrors with radius of curvature 7.8 m. All of them were circular. Prototype No. 4 with diameter 400 mm fulfilled the criteria for the average geometrical quality, but its thickness was 10 mm. Prototype No. 5 with diameter 300 mm and thickness 25 mm had average geometrical quality $s_J = 0.015$ mrad. With increasing mirror diameter and decreasing mirror thickness, the geometrical quality of glass mirrors decreases rapidly. The main reason is decreasing rigidity of the substrate, which changes with the third power of thickness.

Before the first prototypes of LHCb and COMPASS RICH mirrors, twelve former OMEGA mirrors were measured. Results are shown in Fig. 10. The best of them had average geometrical quality $s_J = 0.02$ mrad. Only three had more than 90 % of reflected light inside an angle of 0.03 mrad. By means of optical interference and a microscope objective, we could observe on most OMEGA mirrors deformations of the reflecting surface, see Fig 11. We found correlation between the position of the deformations and the positions of the mounting points at the backside of the mirrors [11].

At present, we use a standard 8-bit CCD camera for the image spot detection. Because of the short dynamic range, we have to detect three spot images at three different, exactly determined light intensities of the point source. A fully automatic program is then looking for the center of gravity of the spot image and measures the amount of light at different diameters. The procedure for finding the center of curvature of the measured mirror was manual. We are preparing a new version of the set-up with

16-bit CCD camera and with a fully automatic procedure for finding the center of curvature. The high dynamic range of the new CCD camera will allow detection of a single spot image per mirror. The measurement precision will be increased and the time, needed for a measurement, will be shortened. Fully automatic measurements are essential when measuring a high numbers of RICH mirrors. To find the center of curvature of the mirror, the spot source and CCD camera will be moved together by means of step-motor controlled by computer. The size of the spot image at different CCD positions will be analyzed and a minimum value found. The center of curvature will be determined at the corresponding position. The automatic procedure will be able to find the position of the center of curvature inside ± 2 mm for R = 8 m.

IV-2 The set-up for mirror local geometrical quality measurement

A new set-up is being prepared, which will probe the topography of the mirror reflective surface. It will enable us to localize its geometrical deformations and deviations. This will contribute to a better understanding of the processes that cause mirror deformations and to find boundaries in size and thickness for this type of mirrors.

IV-2-1 Measurement method

This measurement is based on the modified Shack-Hartmann method [13]. The Shack-Hartmann sensor measures the wavefront distortion after reflection on the measured mirror and its principle is described in Fig. 12. The originally spherical wavefront interacts with the spherical RICH mirror and it is reflected by it. Local deviations of the reflective surface from ideal spherical shape cause corresponding distortions on the reflected wavefront. These distortions are measured by means of a microlens array. Each microlens converts the local angular deviation of the impinging wavefront into a displacement of the corresponding focal spot in the focal plane. The positions of focal spots are detected and their displacements from reference positions are measured. On the basis of these measurements the local deviations of the mirror reflective surface can be analyzed.

IV-2-2 Experimental set-up

The scheme of the set-up is shown in Fig. 13. The set-up is installed on the same optical bench as the set-up described in Sect. IV-1. The point source, located close to the center of curvature of the measured mirror, provides a spherical wavefront. The wavefront is reflected (and at the same time distorted) by the measured mirror. The objective converts (collimates) the spherical wavefront into a plane wavefront. At the plane of the image of the mirror, obtained from the objective, the microlens array is installed (Fig. 13). Finally, the image generated by the microlens array is detected by the CCD camera via the relay lens.

IV-2-3 Experimental results

Although the set-up is in preliminary status, first measurements were performed and analyzed. An important part of the measuring procedure is a program for the automatic measurement of the focal spot displacements.

The result of a preliminary measurement of the LHCb prototype No. 4 is shown in Fig. 14a. The parameters of this circular mirror are indicated in Table 1. The microlens array had a microlens pitch of 400 μm and focal length of 10.7 mm. Some aberration of the mirror is identifiable together with the deformation along one edge (the bottom edge in the picture). For comparison, we measured one of our mirror standards. This is a high quality spherical mirror with the following parameters: made of Simax glass, circular shape, diameter of 400 mm, thickness of 50 mm, radius of curvature of 7.8 m, precision $\lambda/10$. The result is shown in Fig. 14b. The high geometrical quality of this mirror is clearly visible, although a quantitative analysis will require a relatively complex formalism.

IV-3 The set-up for mirror spectral reflectivity measurement

Spectral reflectivity is another RICH mirror parameter that will be measured in the TA2 optical laboratory. We measure in the wavelength range from 200 to 850 nm. In order to minimize mirror manipulation, we incorporate the reflectivity measurement into the same bench as for the previous set-ups. Then each mirror will be installed once and all measurements can be performed consecutively.

The scheme of the set-up is described in Fig. 15. The Xenon pulsed lamp coupled with the solarization resistant optical fiber creates the point source. The measured mirror is illuminated by the point source installed close to the center of curvature of the mirror. Reflected light is focused and injected into another optical fibre coupled with a hand-held spectrometer[7]. The measured values of spectral reflectivity are averages over the whole reflective surface. A radial mapping of reflectivity by means of a variable diaphragm is also envisaged. The Xenon lamp and the spectrometer are synchronized via the computer, which performs the data analysis. The spectrometer is calibrated before measurement to obtain absolute values of the spectral reflectivity.

In the LHCb RICH, the goal is to obtain mirrors from industry with average reflectivity in excess of 85% and with uniformity ±5%.

IV-4 Long-term measurement of the stability of thin spherical mirror geometry

RICH mirrors are large and thin. At present simple glass substrates provide the best results. Since glass is an amorphous medium, creep could affect the long-term geometrical stability of the thin substrate. Creep in regions stressed by forces from gravity or from mounts can cause distortions. To monitor such a process, we will perform a long-term test of mirror geometrical stability. The prototype will be fixed on the prototype of the mount, in the same position as inside the detector vessel. The

[7] From Ocean Optics, model S2000 Spectrometre

main parameters of the mirror will then be measured regularly. We will measure the mirror geometry by means of the previously described set-ups.

V CONCLUSIONS

In the past two years, an optical laboratory was initiated and it is now routinely run by our group. Its main task consists in studying, characterizing and qualifying optical elements for future RICH- and other optically-based particle detectors.

In the framework of the RICH project for the LHCb detector, we have characterized about forty mirror prototypes. Their geometrical quality has been improving with time and the measurements performed on them allow us to conclude that mirrors with a Simax glass substrate, a thickness of 6 to 7 mm, a radius of curvature of 8 m and an ascribed diameter up to ~500 mm are feasible with the geometrical requirement of s_J = 0.03 mrad. That is, they are capable of focussing 95% of the reflected light into a circle with diametre D_0 = 2 mm at the plane defined by the mirror radius of curvature R = 8 m.

Finally, two effects on the mirror geometrical quality have to be yet carefully analyzed : the influence of the final mirror mount and the mirror long-term behaviour.

ACKNOWLEDGEMENTS

We would like to thank our collaborators in the group for the logistic and technical support. We acknowledge the stimulating environment of the LHCb – RICH project team. We also thank mirror producers: COMPAS R&D Consortium, Turnov; Glass Mountain Optics, Austin, Texas; Optical Works Ltd, England.

REFERENCES

[1] The LHCb Collaboration, “Technical Proposal”, CERN/LHCC 98-4, LHCC/P4 (1998); D. Websdale, on behalf of the LHCb Collaboration, 1999;

[2] V. Obratzov, V. Polyakov, Private Communication;

[3] O. Ullaland et al., LHCb RICH-2 Mechanics, LHCb Technical Note 2000-xx;

[4] C. D’Ambrosio, M. Laub, D. Piedigrossi, P. Wertelaers, P. Wicht, “An experimental set-up to measure the long-term stability of large-mirror supports”, LHCb Technical Note 2000-20, 18 april 2000;

[5] C. D’Ambrosio, M. Laub, D. Piedigrossi, P. Wertelaers, P. Wicht, “Characterization of mirror mount prototypes for RICH detectors”, LHCb Technical Note 2000-xx;

[6] G. Baum et al., *The COMPASS RICH1 Detector*, Nuclear Physics B (Proc. Suppl.) 78 (1999) 345-359;

[7] C. D’Ambrosio, M. Laub, D. Piedigrossi, “Optical qualification of the first COMPASS RICH mirrors”, COMPASS Technical Note, 2000-4, 17 march 2000;

[8] M. Born, E. Wolf, “Principles of Optics”, Pergamon, Oxford, (1970);

[9] S. Solimeno, B. Crosignani, P. Di Porto, “Guiding, Diffraction and Confinement of Optical Radiation”, Academic Press Inc., ISBN 0-12-653341-0 (1986);

[10] M. Atkinson et al., *A proposal to build a ring image Cerenkov detector for use by the Omega Photon Collaboration in WA69 (P231)*, Internal note, April 1982;M. Laub, COMPASS RICH Presentation, July 1999;

[11] T. Korhonen et al., *Hartmann interferometric testing of large mirrors*, SPIE Vol. 1531 Advanced Optical Manufacturing and Testing II (1991);

Table 1: Parameters of measured mirror prototypes and mirrors.

Mirror	Shape	Coating	Diameter [mm]	Thick. [mm]	R^* [m]	D_0 [mm]	σ_ϑ [mrad]
COMPASS proto 1	Hex.	No	520	7	6.0	1.95	0.040
COMPASS proto 2	Circ.	No	600	8	6.6	2.55	0.048
COMPASS proto 3	Circ.	No	600	8	6.6	-	-
COMPASS proto 4	Hex.	No	540	8	6.6	2.12	0.040
COMPASS proto 5	Hex.	No	540	7.5	6.6	1.44	0.027
COMPASS 1	Hex.	No	520	7	6.6	2.22	0.042
COMPASS 2	Hex.	No	520	7	6.6	2.91	0.055
COMPASS 3	Hex.	No	520	7	6.6	2.39	0.045
COMPASS 4	Hex.	No	520	7	6.6	4.02	0.076
COMPASS 5	Hex.	No	520	7	6.6	1.79	0.034
COMPASS 6	Hex.	No	520	7	6.6	2.56	0.048
COMPASS 7	Hex.	No	520	7	6.6	2.65	0.050
COMPASS 8	Hex.	No	520	7	6.6	2.82	0.053
COMPASS 9	Hex.	No	520	7	6.6	1.71	0.032
COMPASS 10	Hex.	No	520	7	6.6	2.31	0.044
COMPASS 0	Hex.	No	520	6	6.6	1.39	0.026
LHCb proto 1	Circ.	No	340	8.5	7.8	2.46	0.039
LHCb proto 2	Circ.	No	400	7.5	7.8	3.40	0.054
LHCb proto 3	Circ.	Yes	340	7	7.8	-	-
LHCb proto 4	Circ.	No	400	10	7.8	1.95	0.031
LHCb proto 5	Circ.	Yes	300	25	7.8	0.93	0.015
Best OMEGA	Hex.	Yes	430	50**	10.0	1.53	0.019

* Nominal values

** OMEGA mirrors are sandwich type with glass-foam

Table 2: Results of radius of curvature R and of diameter D_0 measurements for COMPASS mirrors.

Mirror	R [mm]	D_0 [mm]	s_J [mrad]
COMPASS 1	6620	2.22	0.042
COMPASS 2	6639	2.91	0.055
COMPASS 3	6654	2.39	0.045
COMPASS 4	6607	4.02*	0.076*
COMPASS 5	6653	1.79	0.034
COMPASS 6	6660	2.56	0.048
COMPASS 7	6605	2.65	0.050
COMPASS 8	6632	2.82	0.053
COMPASS 9	6637	1.71	0.032
COMPASS 10	6583	2.31	0.044
Average	6629	2.37	0.045
Std. Dev.	25	0.42	0.008

*This value was not considered in the average and std. dev. calculations

Table 3: Results of radius of curvature R and of diameter D_0 measurements for COMPASS mirror No. 0, placed each time on the mirror holder varying its edge position.

Position	R [mm]	D_0 [mm]	s_J [mrad]
A	6642	1.45	0.027
B	6645	1.20	0.023
C	6644	1.54	0.029
D	6644	1.62	0.031
E	6647	1.28	0.024
F	6647	1.20	0.023
A(2)	6642	1.45	0.027
Average	6644.43	1.39	0.026
Std. Dev.	2.07	0.17	0.003

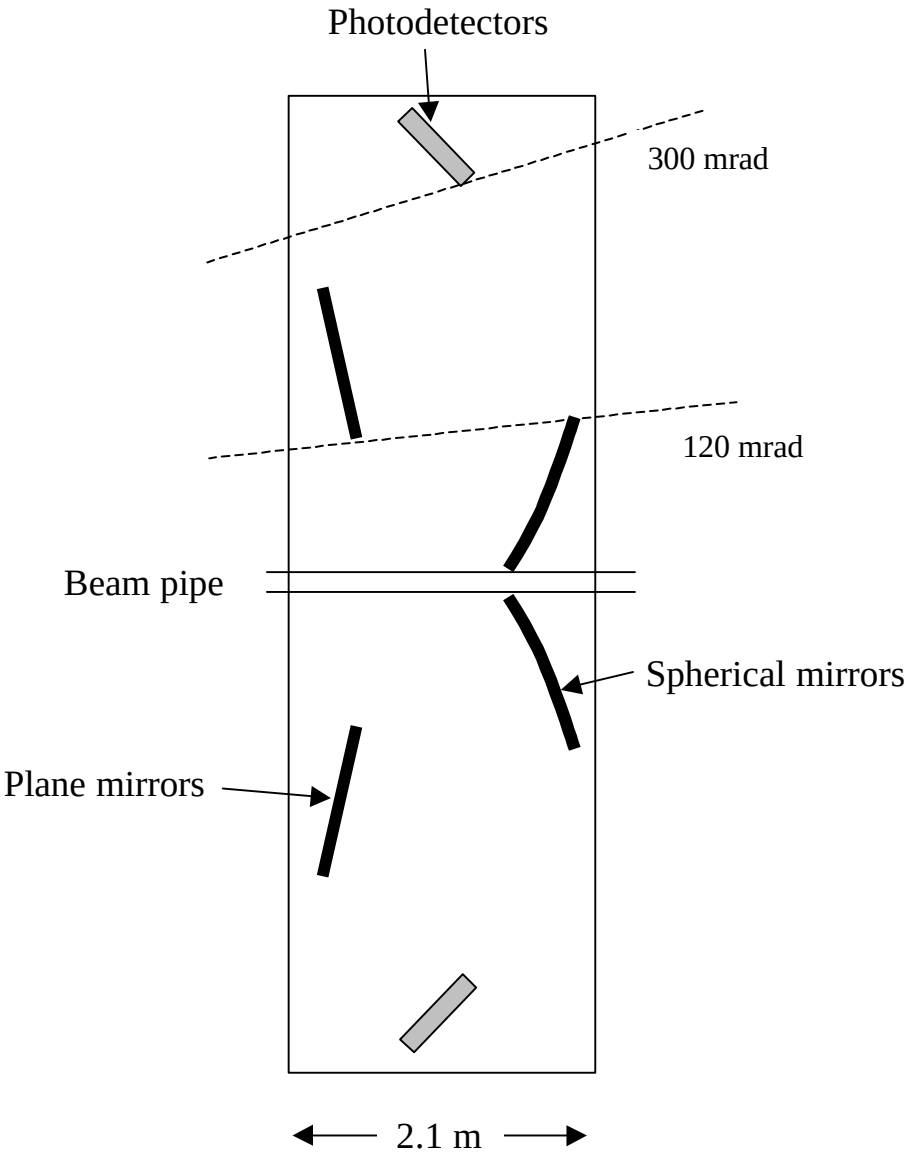

Fig. 1: LHCb RICH-2 main optical components and their positions.

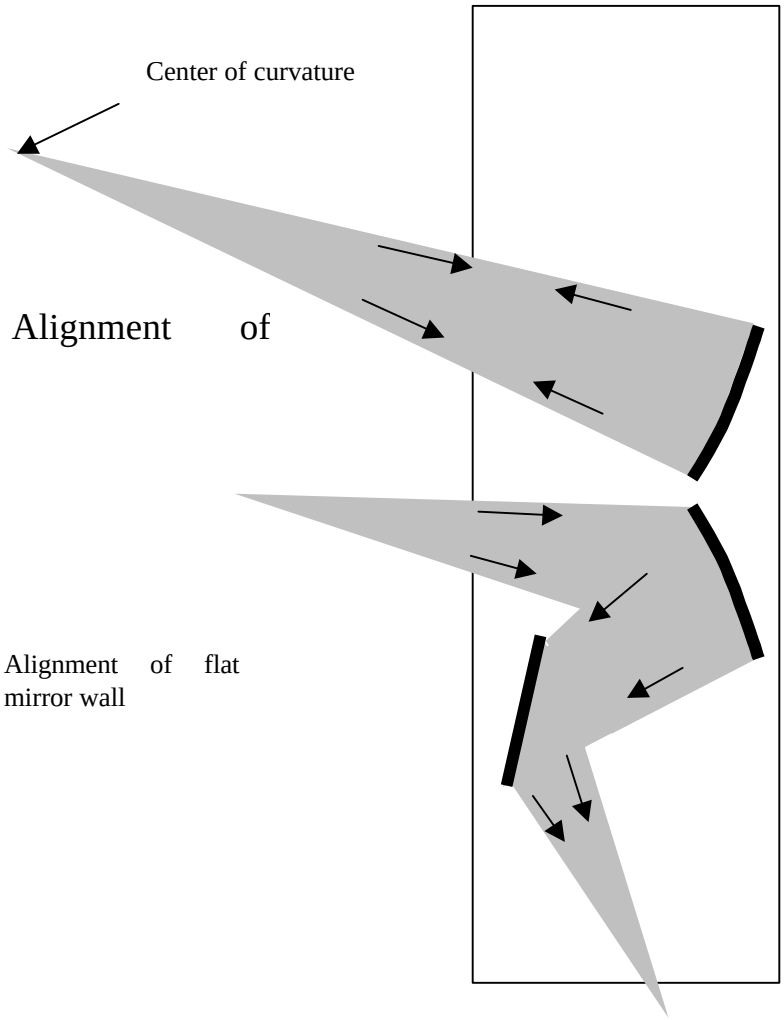

Not to scale

Fig. 2: Laser alignment procedure for spherical and flat mirror walls. First the spherical wall is aligned, by means of a point source placed in the center of curvature of the wall, defined by survey. Then the flat panel is mounted and aligned by moving the point source to a proper position near the beam axis and using its image point.

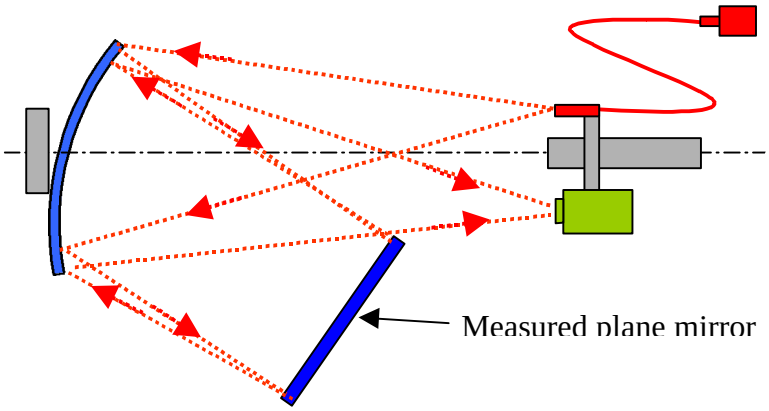

Three points mirror holder

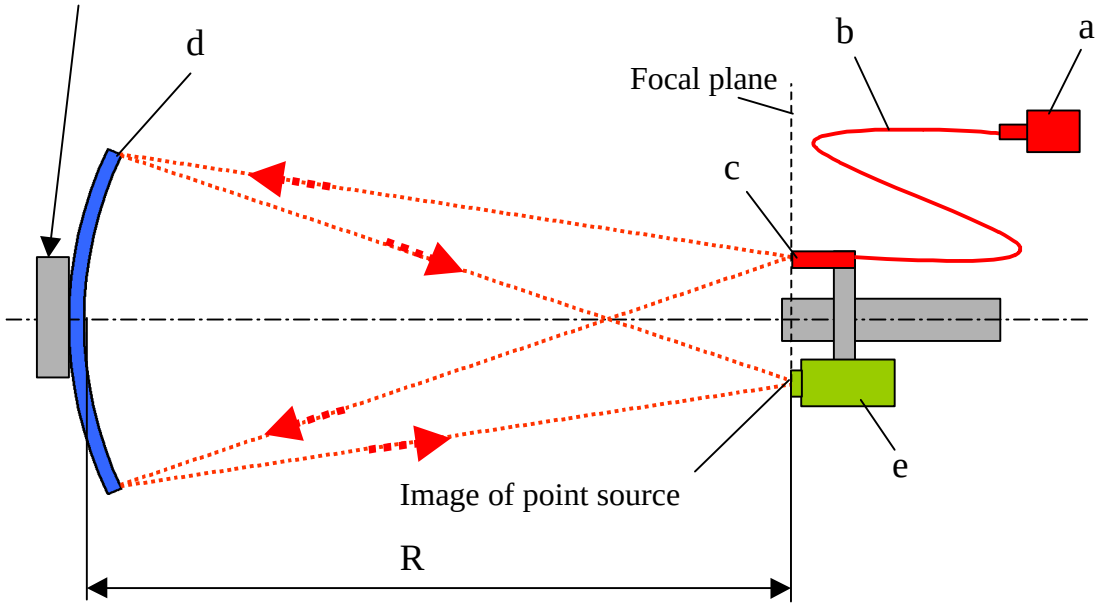

Not to scale

Fig. 3: Set-up for spherical mirror radius of curvature and average geometrical quality measurement. At the top: modification for flat mirror measurement.

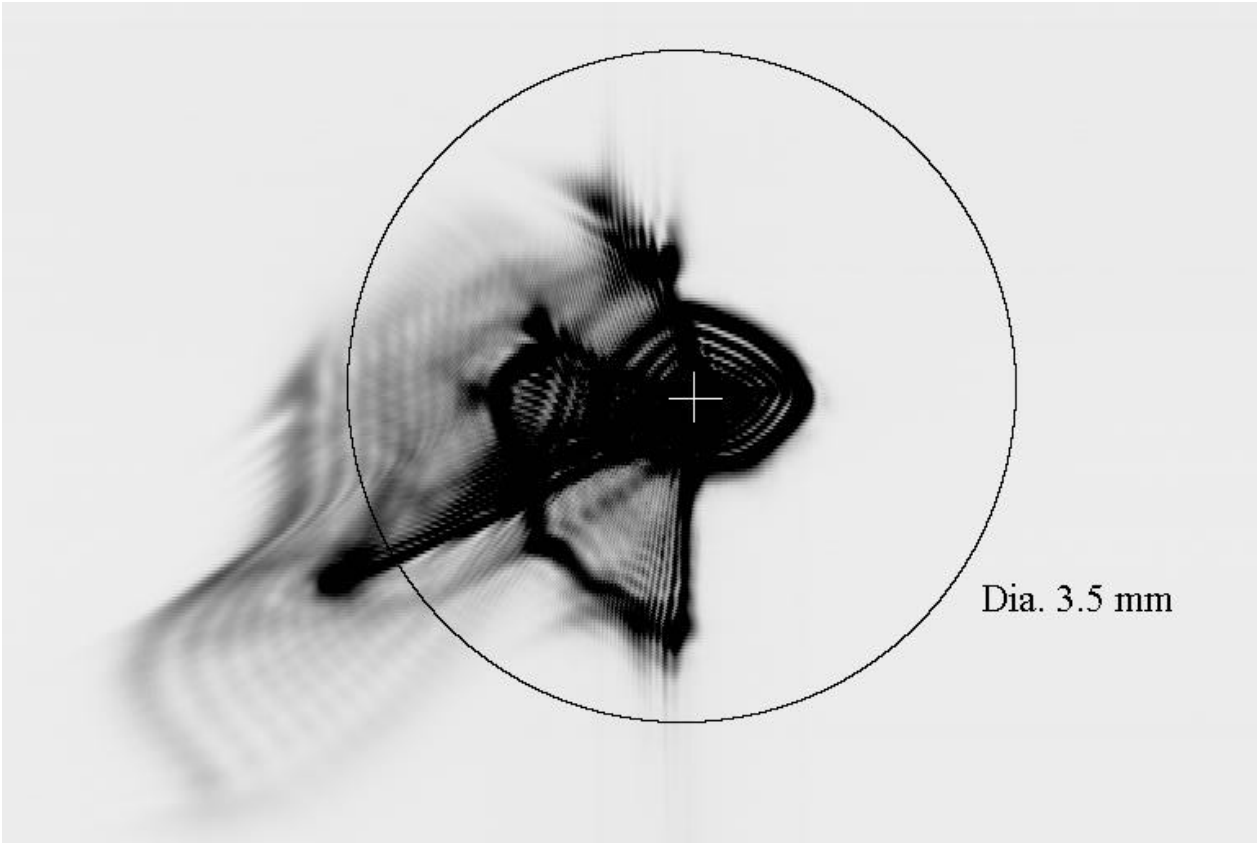

Fig. 4: Spot image of COMPASS mirror No. 4. The image is overexposed to show low intensity regions.

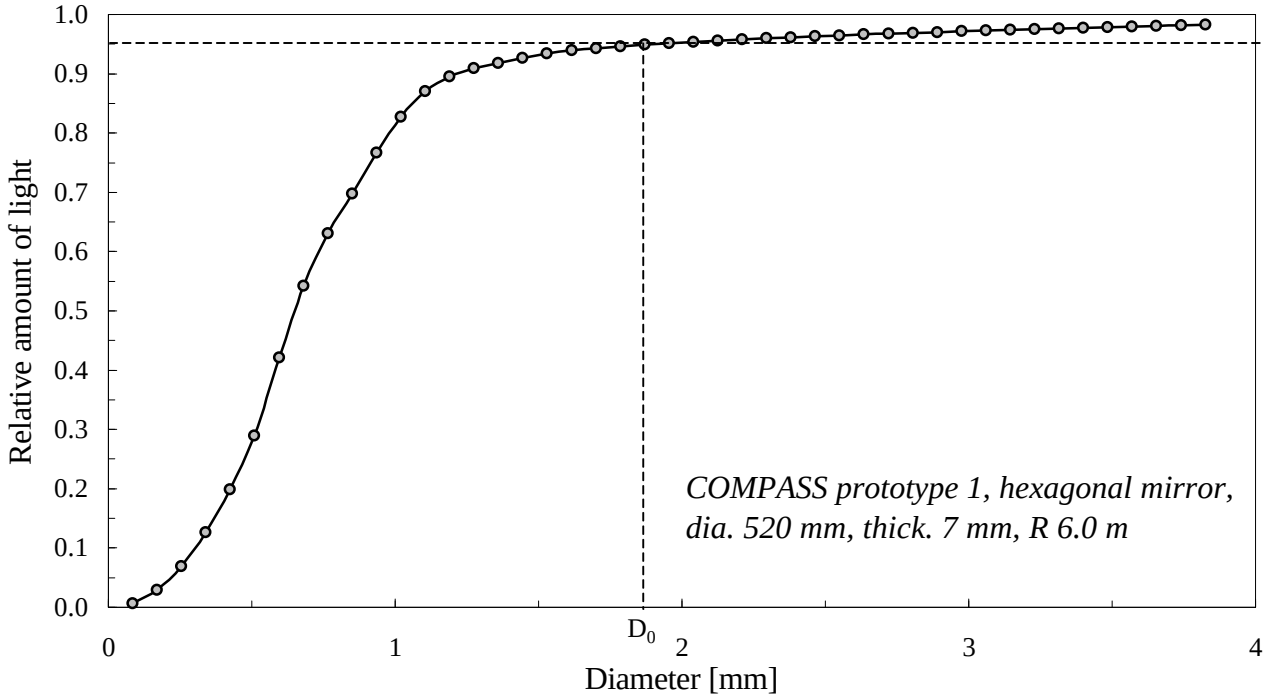

Fig. 5: Light fraction inside a circle with diameter *D*. Shown is the corresponding D_0.

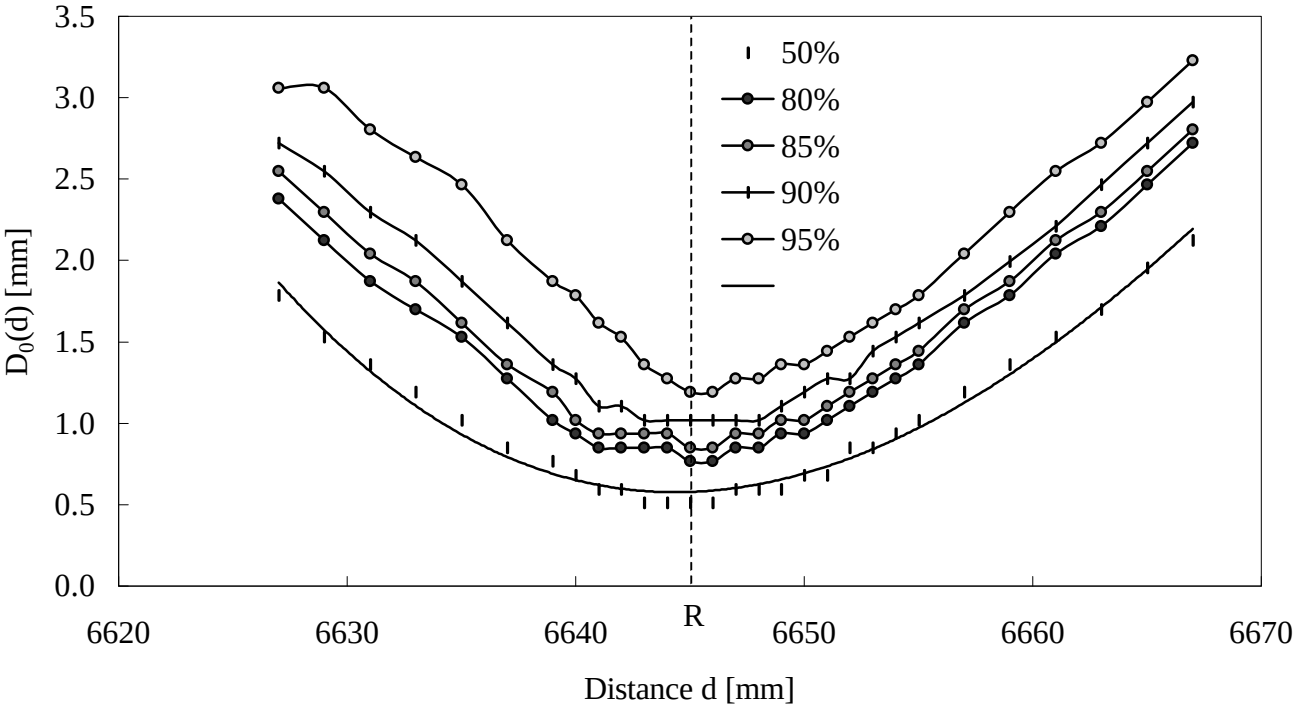

Fig. 6: Spot size vs. distance d for COMPASS mirror No. 0. It shows the procedure for the center of curvature finding and that the minimum spot size stays the same for different circles containing different fractions of light. For the 50% curve, an hyperbolic curve is shown, which fits well the data. This would not be the case for the 95% curve, showing that the spot is not gaussian.

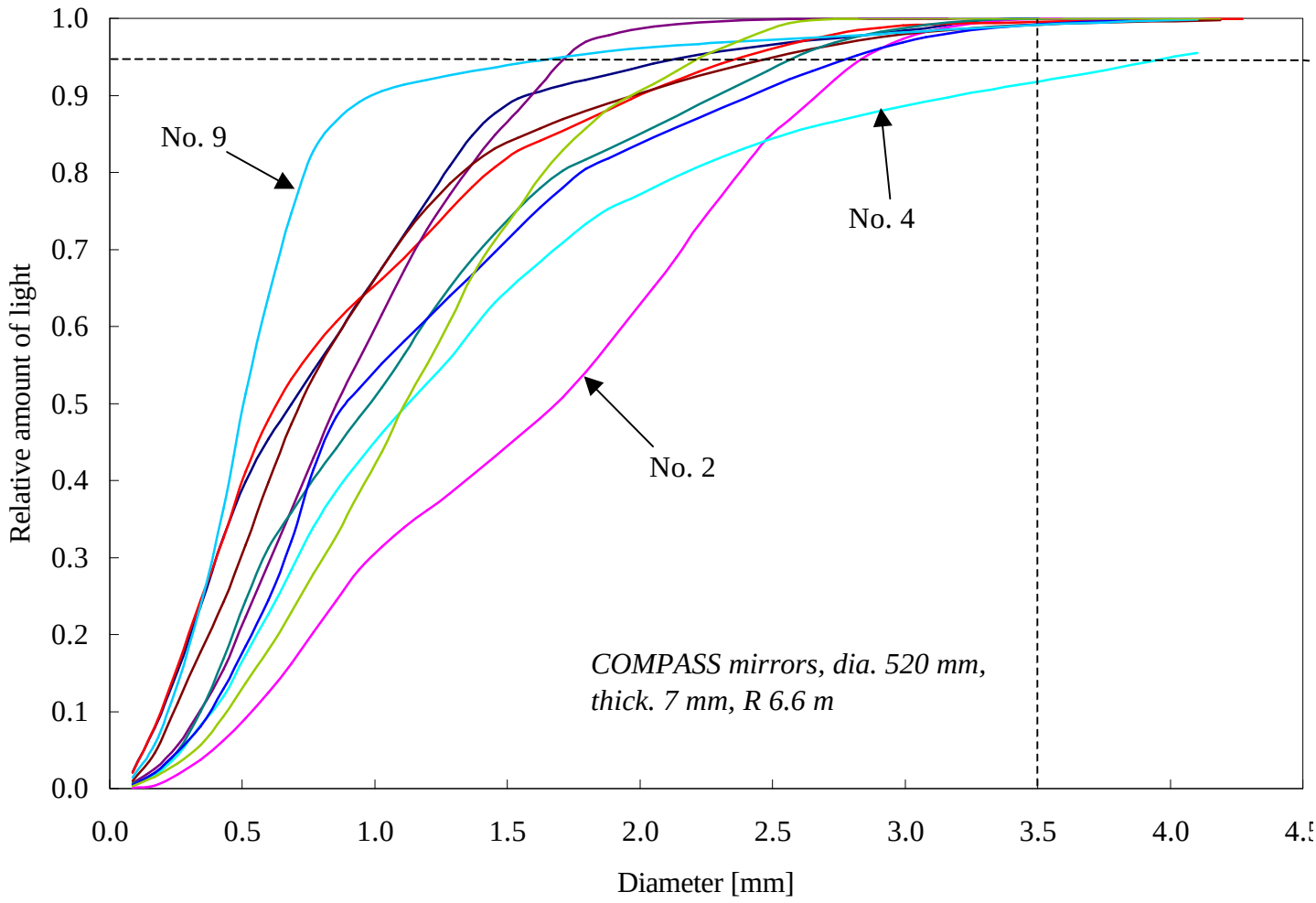

Fig. 7: Light fraction inside a circle at different diameters. Results for the first ten COMPASS mirrors.

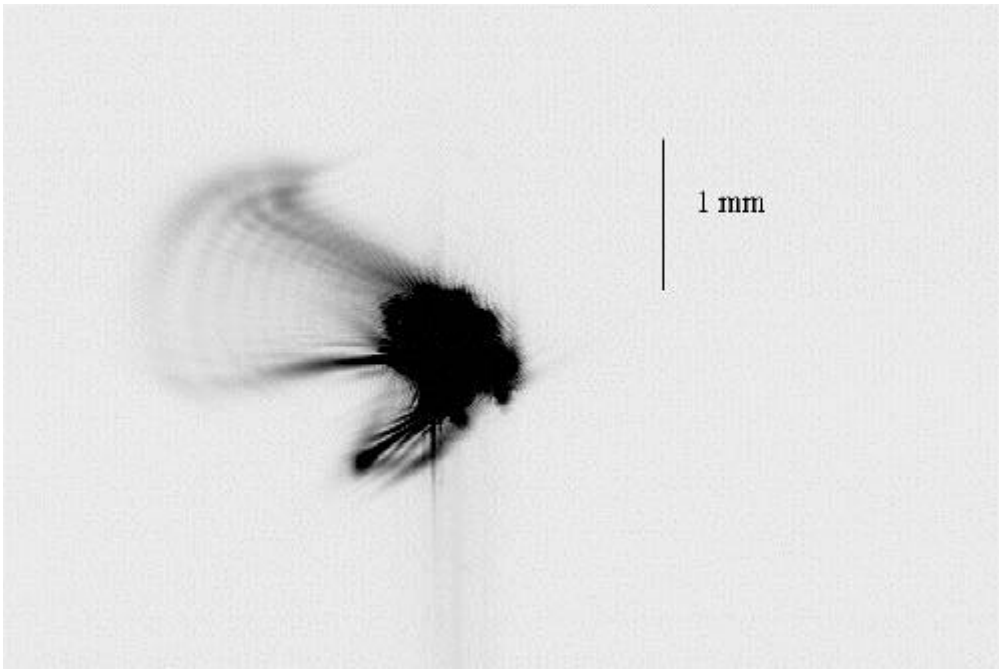

Fig. 8a: Spot image from COMPASS mirror No. 9.

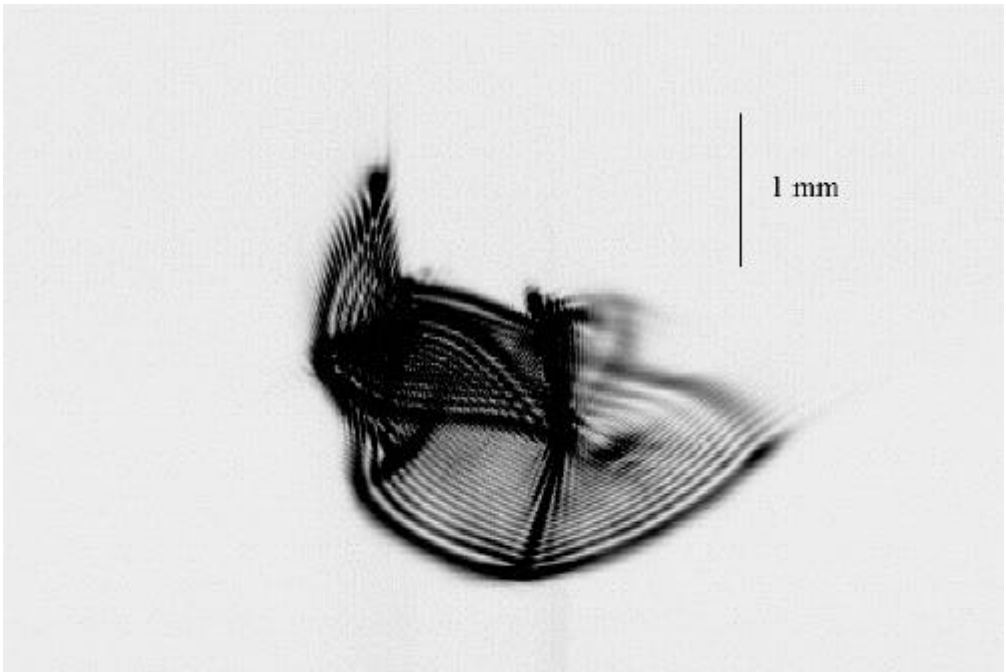

Fig. 8b: Spot image from COMPASS mirror No. 2.

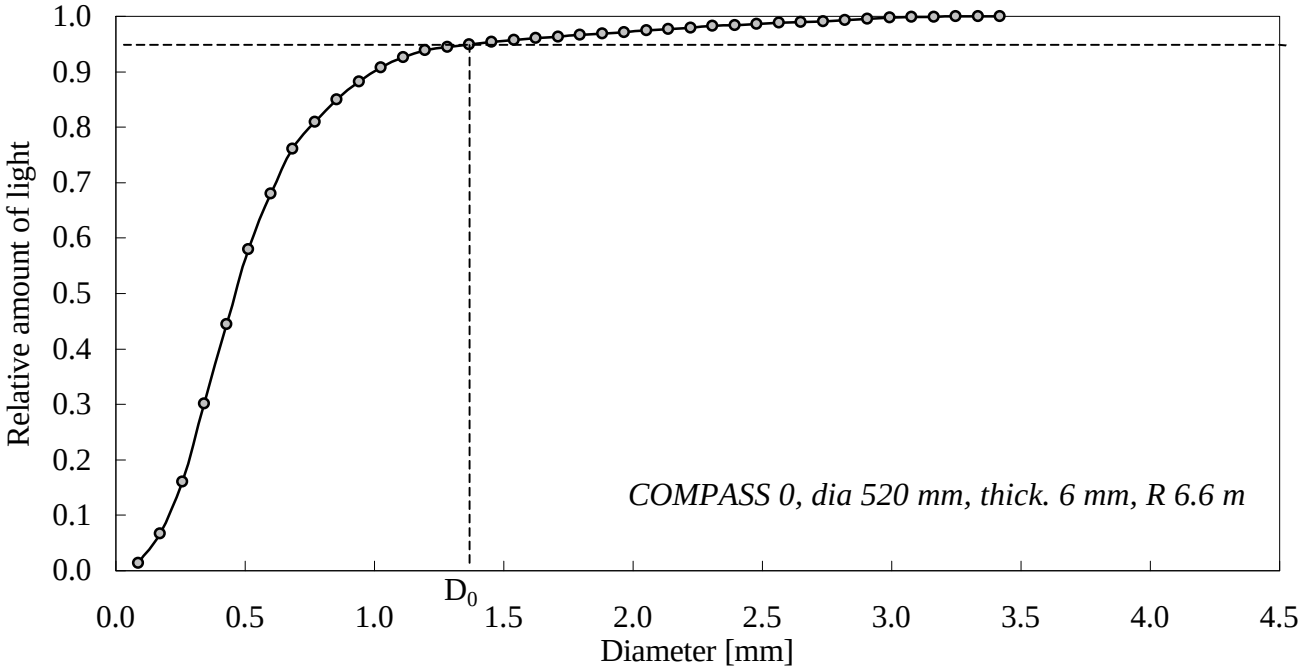

Fig. 9: Light fraction inside a circle at different diameters. Shown is the corresponding D_0.

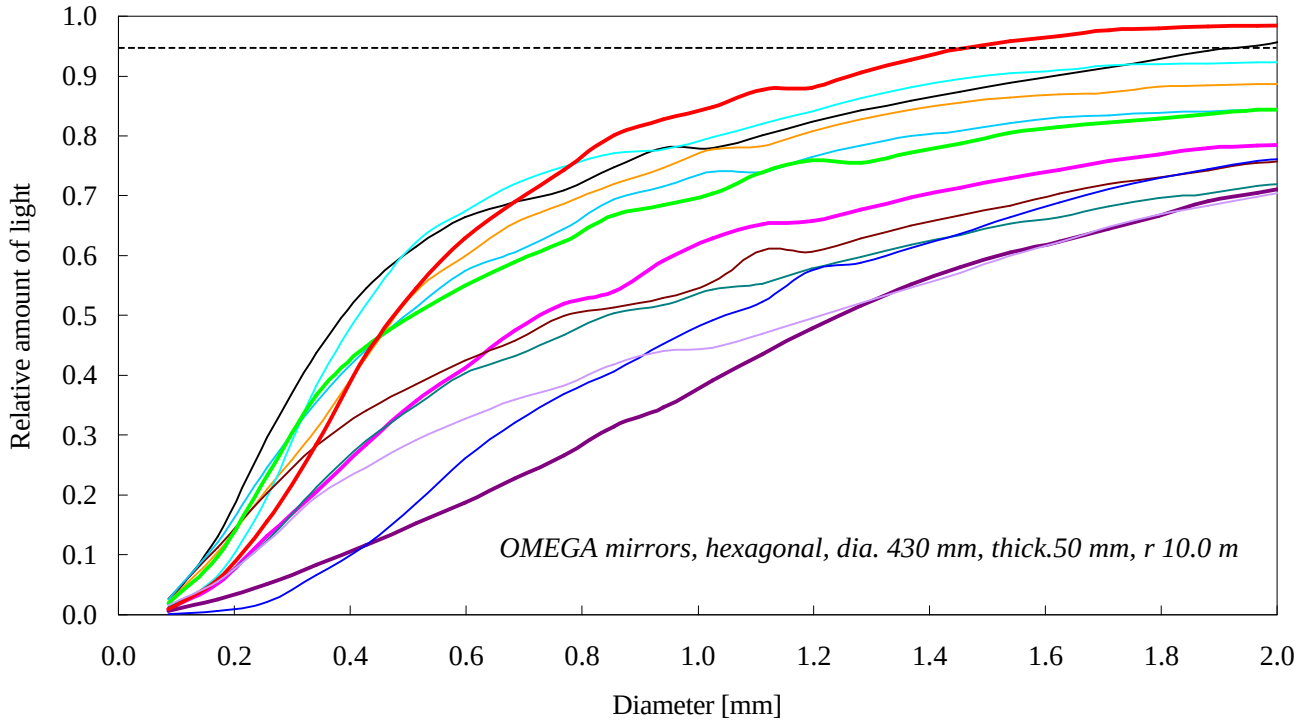

Fig. 10: Light fraction inside a circle at different diameters. Results from twelve OMEGA mirrors.

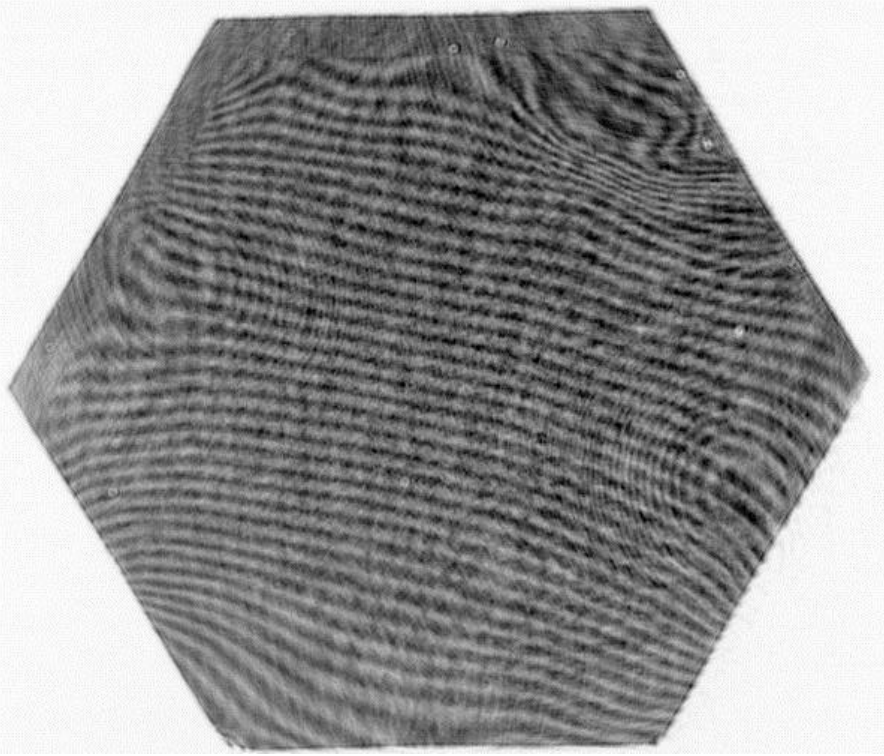

Fig. 11a: OMEGA No. 10. No big fault.

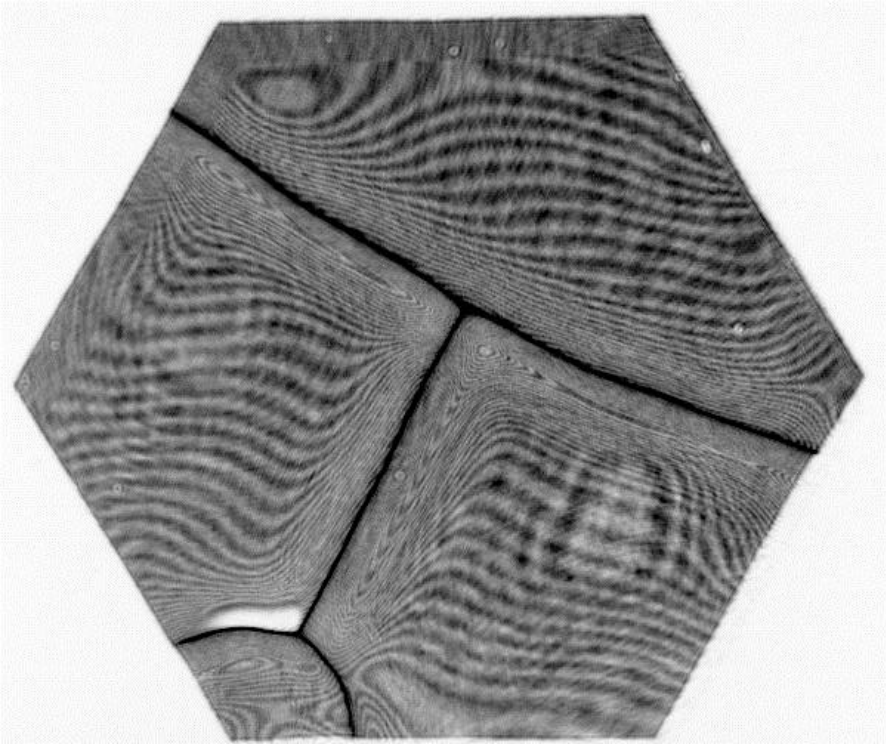

Fig. 11b: OMEGA No. 5. Deformations correspond to mounts on back side.

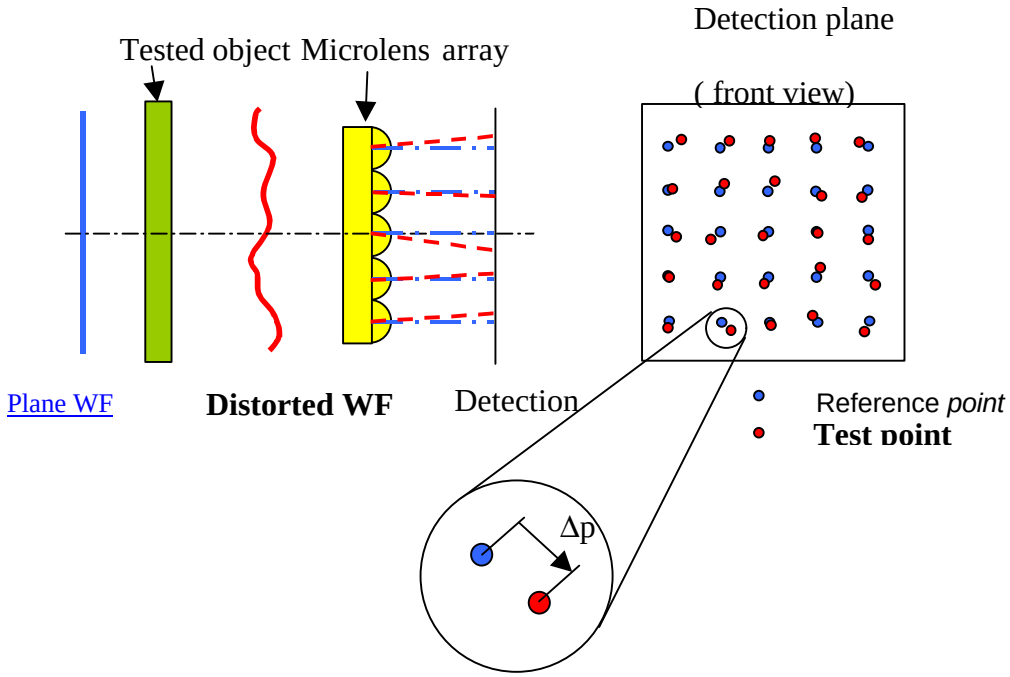

Fig. 12: Principle of Shack-Hartmann sensor.

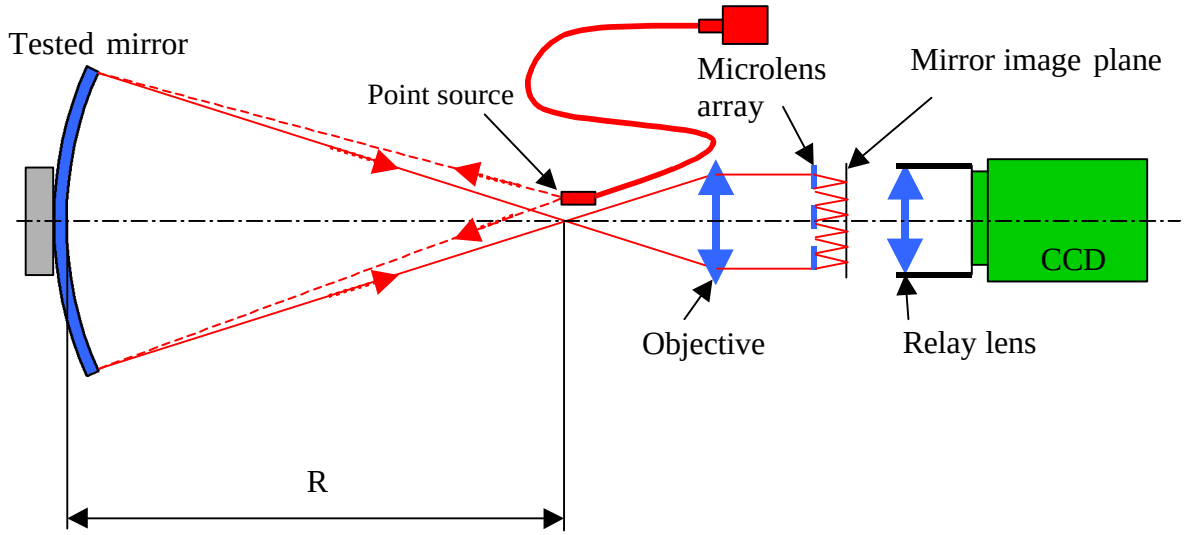

Fig. 13: Scheme of set-up for mirror local geometrical quality measurement.

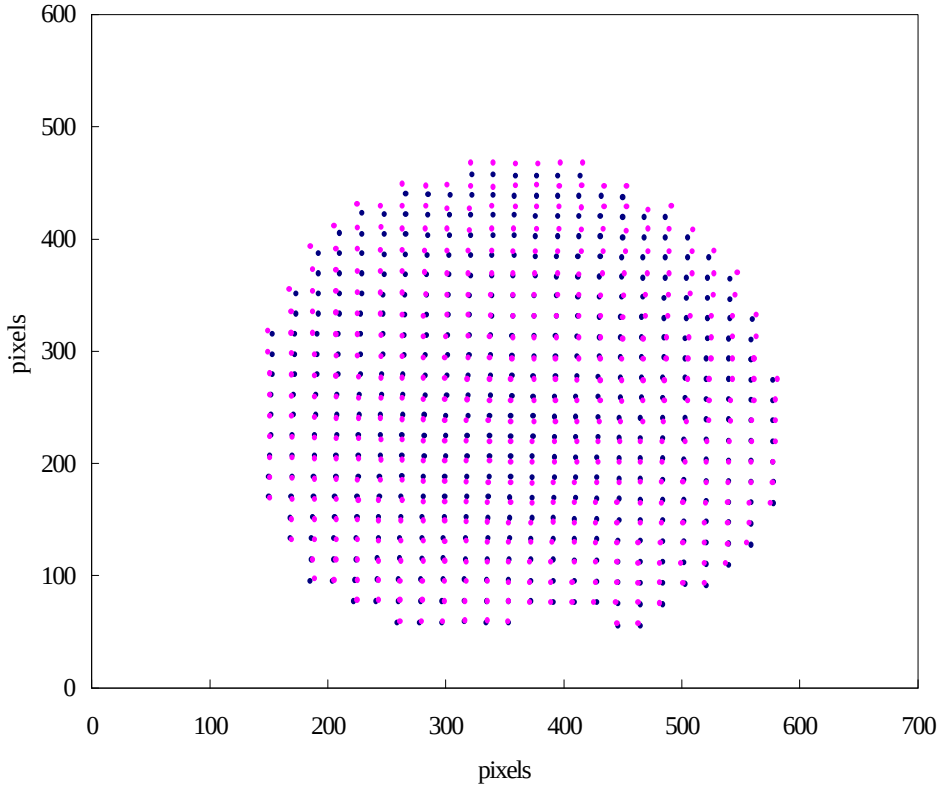

Fig. 14a: Preliminary measurement of LHCb prototype NO. 4.

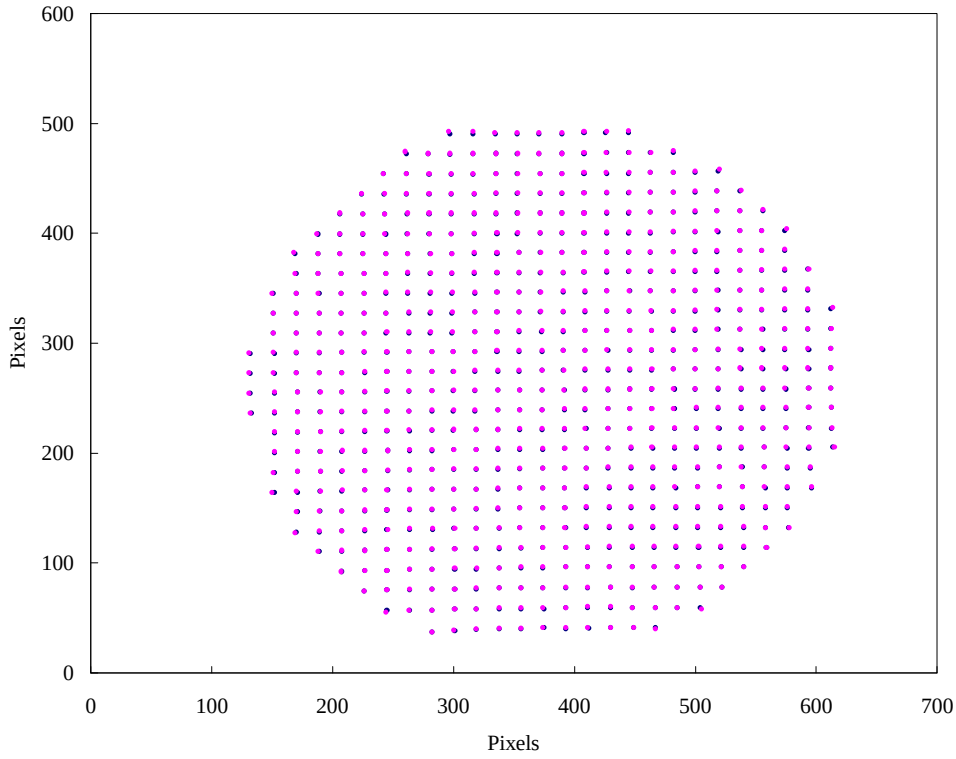

Fig. 14b: Preliminary measurement of mirror standard.

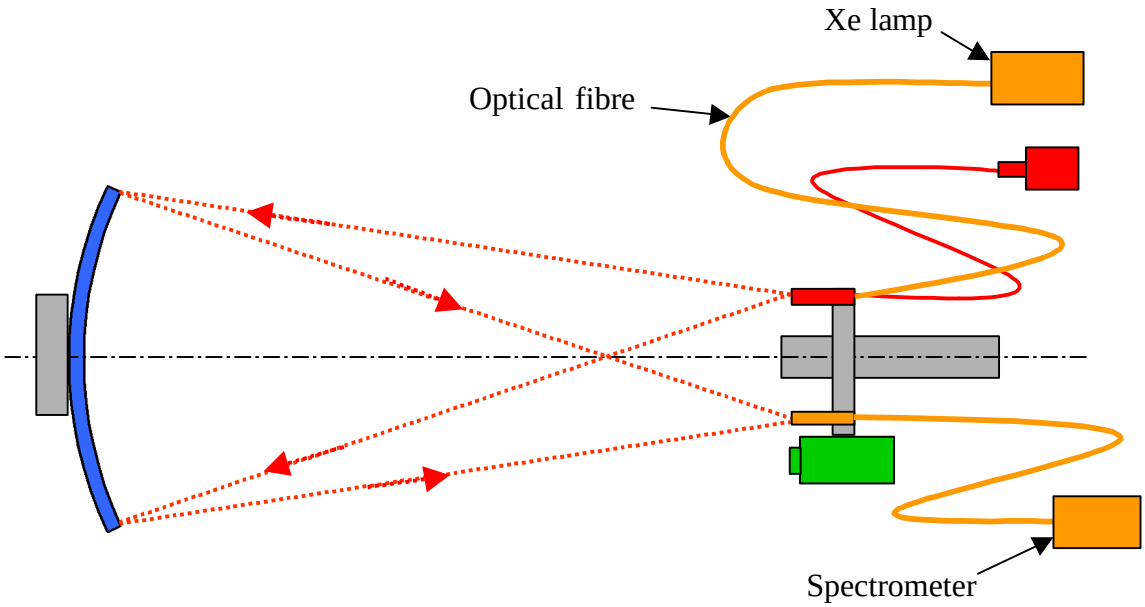

Fig. 15: Scheme of set-up for mirror average spectral reflectivity measurement.